J Ind Microbiol Biotechnol (2015) 42:585–600
DOI 10.1007/s10295-015-1588-7

FERMENTATION, CELL CULTURE AND BIOENGINEERING

SIMB
Society for Industrial Microbiology and Biotechnology

Quantifying the sensitivity of *G. oxydans* ATCC 621H and DSM 3504 to osmotic stress triggered by soluble buffers

B. Luchterhand · T. Fischöder · A. R. Grimm · S. Wewetzer · M. Wunderlich · T. Schlepütz · J. Büchs

Received: 25 November 2014 / Accepted: 14 January 2015 / Published online: 3 February 2015

Abstract In *Gluconobacter oxydans* cultivations on glucose, $CaCO_3$ is typically used as pH-buffer. This buffer, however, has disadvantages: suspended $CaCO_3$ particles make the medium turbid, thereby, obstructing analysis of microbial growth via optical density and scattered light. Upon searching for alternative soluble pH-buffers, bacterial growth and productivity was inhibited most probably due to osmotic stress. Thus, this study investigates in detail the osmotic sensitivity of *G. oxydans* ATCC 621H and DSM 3504 using the Respiratory Activity MOnitoring System. The tested soluble pH-buffers and other salts attained osmolalities of 0.32–1.19 osmol kg^{-1}. This study shows that *G. oxydans* ATCC 621H and DSM 3504 respond quite sensitively to increased osmolality in comparison to other microbial strains of industrial interest. Osmolality values of >0.5 osmol kg^{-1} should not be exceeded to avoid inhibition of growth and product formation. This osmolality threshold needs to be considered when working with soluble pH-buffers.

Keywords *Gluconobacter oxydans* · pH-buffer systems · Water activity · Osmotic pressure · RAMOS

Electronic supplementary material The online version of this article (doi:10.1007/s10295-015-1588-7) contains supplementary material, which is available to authorized users.

B. Luchterhand (✉) · S. Wewetzer · M. Wunderlich · T. Schlepütz · J. Büchs
AVT, Chair of Biochemical Engineering, RWTH Aachen University, Worringerweg 1, 52074 Aachen, Germany
e-mail: bettina.luchterhand@avt.rwth-aachen.de

J. Büchs
e-mail: Jochen.Buechs@avt.rwth-aachen.de

T. Fischöder
Department of Biotechnology/Biomaterial Sciences and Helmholtz Institute for Biomedical Engineering, RWTH Aachen University, Pauwelsstr. 20, 52074 Aachen, Germany

A. R. Grimm
Institute of Biotechnology, RWTH Aachen University, Worringerweg 3, 52074 Aachen, Germany

Introduction

Gluconobacter oxydans, an acetic acid bacterium, is interesting for various industrial applications, because it can partially oxidize a variety of sugars and alcohols. With D-glucose as substrate, *Gluconobacter* strains are able to produce D–gluconate (GA), 5–ketogluconate (5KGA), 2–ketogluconate (2KGA) and 2, 5–diketogluconate (DKGA). D–gluconate and its salts are applied in several industries, e.g., in the textile and tanning sector and in the pharmaceutical, fodder, and concrete industries [21]. With a production of 10,000 t/a, GA is one of the top-ten organic chemicals made from sugar [25]. To oxidize GA, *G. oxydans* expresses two types of gluconate dehydrogenases: (1) quinoprotein glycerol (major) dehydrogenase for 5KGA production, and (2) flavoprotein for 2KGA production. The fermentation product 5KGA is a precursor for L(+)–tartaric acid production. Moreover, 2KGA can further be converted to DKGA via the membrane-bound NADP-independent 2KGA dehydrogenase in *G. oxydans* [20]. Subsequently, DKGA can be reduced to 2–keto–L–gulonate, e.g., with *Corynebacterium* species [45]. The product 2–keto–L–gulonate is a precursor for the industrial production of ascorbic acid, commonly known as vitamin C.

The different membrane-bound dehydrogenases in *G. oxydans* possess different specific pH-optima. A pH-value of around 6 was found to be optimal for the membrane-bound D-glucose dehydrogenase and the D–gluconate

dehydrogenase [1, 26, 42]. By contrast, 2–ketogluconate dehydrogenase showed the highest enzymatic activity at a pH-value of 4 [41]. In unbuffered cultivations of *G. oxydans*, however, the efficient oxidation of D–glucose to gluconic acids leads to a strong drop in the pH-value below 2.5, which clearly deviates from the optima for the dehydrogenases.

Although *G. oxydans* strains show optimal growth at pH-values between 5.5 and 6 [20], most strains are still able to grow at pH-values below 3.7. As shown by Olijve and Kok [30], *G. oxydans* 621H even grows in complex medium at a constant pH-value of 2.5. Yet, at pH-values below 3.5, the pentose phosphate pathway (PPP) in *G. oxydans* is completely inhibited [30]. The PPP is one of the two main metabolic pathways in *G. oxydans* and is considered to be the most important route for the assimilation of sugars and polyols to CO_2 and biomass [5]. Thus, an inactivated PPP results in low biomass formation [30].

Since the pH-value has a considerable impact on cell growth and product formation of *G. oxydans*, the pH has to be controlled during fermentation. While pH-control in stirred bioreactors can easily be realized via titration [31], keeping a specific pH-value in small-scale cultivations is challenging. For pH-control in shake flasks, Weuster-Botz et al. [48, 49] and Zou et al. [52] presented systems for adding pH-control agents. Here, the required equipment, i.e., pH probes, storage vessels and pumps, makes these systems complex and impractical for high-throughput applications. Buchenauer et al. [9] and Funke et al. [14] proposed a microfluidic approach for the 48-well microtiter plate format to add pH-control agents with an accuracy of 5 nL dispensed volume. Based on this concept, a commercial device has been developed by m2p-labs (Baesweiler, Germany) offering 32 parallel, fully monitored bioreactors with two feeding options each. However, this device is also not suited for high-thoughput.

Commonly for shake flasks and MTPs a buffer reagent is added to the medium to keep the pH-value within a certain range during the cultivation [20, 35, 38, 44]. To prevent a strong drift of the pH-values, these buffers are highly concentrated and, thus, result in high osmolalities of the fermentation medium [22, 24].

Often, shake flask cultivations of *G. oxydans* are buffered with $CaCO_3$ [6, 20]. Since $CaCO_3$ is nearly insoluble in water, its suspended particles hinder analysis of optical density and scattered light measurements for biomass determination during cultivations [44, 51]. Furthermore, $CaCO_3$ complicates the determination of dry cell weight (DCW). The application of soluble buffers could overcome these disadvantages.

In the search for soluble buffers, the inherent increase in osmolality of the fermentation medium has to be considered. This increase in osmolality causes osmotic stress, possibly inhibiting bacterial growth and product formation [7, 27]. Thus, the aim of this study is to investigate in detail the osmotic sensitivity of wildtype strains *G. oxydans* ATCC 621H and DSM 3504. Bacterial growth in various soluble buffer systems was characterized using the Respiration Activity MOnitoring System (RAMOS). Moreover, to investigate the effect of osmotic stress on the *G. oxydans* strains, defined amounts of salts (NaCl, KCl or $MgSO_4$) were added to $CaCO_3$-buffered medium before the cultivations.

Material and methods

Chemicals

Applied chemicals were obtained from Merck (Darmstadt, Germany), Sigma-Aldrich (Hamburg, Germany), Carl Roth (Karlsruhe, Germany) and Boehringer Mannheim (Mannheim, Germany).

Microorganisms

Experiments were conducted with *G. oxydans* wildtype strains ATCC 621H and DSM 3504 (equivalent to DSM 2343). Both strains possess a natural resistance against cefoxitin. In contrast to strain DSM 3504, strain ATCC 621H cannot produce DKGA due to the lack of the gene encoding the membrane-bound 2KGA dehydrogenase [40, 47]. Strains were maintained in 15 % (w/v) glycerol cryo stocks at −80 °C.

Media and cultivation

Pre-cultures of *G. oxydans* DSM 3504 and ATCC 621H were grown in a complex mannitol medium containing 80 g L^{-1} mannitol, 5 g L^{-1} yeast extract, 2.5 g L^{-1} $MgSO_4 \cdot 7H_2O$, 1 g L^{-1} KH_2PO_4 and 1 g L^{-1} $(NH_4)_2SO_4$. Ten milliliter of the complex mannitol medium and 10 µL cefoxitin (50 mg mL^{-1} stock solution) were inoculated with 1 mL of a cryo-stock culture in a 250 mL non-baffled shake flask. The cultivation was performed 15–17 h overnight at 30 °C, 350 rpm shaking frequency and 50 mm shaking diameter.

Main cultivations of *G. oxydans* DSM 3504 and ATCC 621H were conducted in complex glucose medium composed of 40 g L^{-1} (222 mmol L^{-1}) glucose, 5 g L^{-1} yeast extract, 2.5 g L^{-1} $MgSO_4 \cdot 7H_2O$, 1 g L^{-1} KH_2PO_4 and 1 g L^{-1} $(NH_4)_2SO_4$. The pH-value was adjusted to 6 with KOH or HCl (1 M each). Buffer characterizations were performed using 0.22 mol L^{-1} of different soluble buffers and $CaCO_3$ as reference (Table 1). To investigate the influence of osmotic stress on *G. oxydans*, varying amounts of NaCl, KCl or $MgSO_4$ were added, respectively, to the

Table 1 Overview of the investigated buffer systems with their molecular structures, molecular weights and specific pK_a values[a]

Buffer system	Molecular structure	M [g mol^{-1}]	pK_a (30°C)	References
Lime	$CaCO_3$	100.09	6.33 (10.29)	[13,16]
MES (2-(N--morpholino)-ethane sulphonic acid	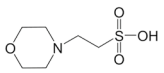	195.2	6.1	[23]
PIPPS (Piperazine-1,4--bis(propanesulphonic acid	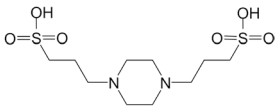	330.42	3.72 (7.9)	[23]
Citric acid	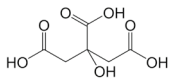	192.13	3.13 4.75 6.4	[13,16]
Phthalic acid	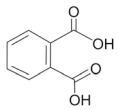	204.22	4.02	[13,16]
DEPP (1,4-diethylpiperazine acid)	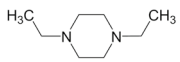	142.24	4.46 (8.61)	[23]

pK_a values above 6, which are not relevant for the employed pH-range, are indicated in brackets

[a] The specific pK_a values at 30 °C were calculated as described in the references specified below

medium buffered with 0.22 mol L^{-1} $CaCO_3$. All media were autoclaved for 21 min at 121 °C. Since $CaCO_3$ is insoluble in the fermentation medium, the required amount was weighed and added directly into the shake flasks prior to their sterilization.

To obtain an initial optical density of 0.1 in the main culture, the optical density at 600 nm (OD_{600}) of the pre-culture was determined in a Genesys 20 photometer (Thermo Scientific, Dreieich, Germany), and the required volume of cell broth was calculated. The required volume was centrifuged (10,000×*g*, 5 min) in a sterile centrifugation tube and the supernatant was discarded. Subsequently, the cell pellet was re-suspended in the main culture medium. Aliquots of 10 mL inoculated medium were transferred to each flask and the cultivations performed at 30 °C, 350 rpm shaking frequency and 50 mm shaking diameter.

Measurement of respiration activity

Online-monitoring of the respiration activity was performed with an in-house developed RAMOS device. RAMOS enables measurements of oxygen transfer rate (OTR), carbon dioxide transfer rate (CTR) and respiratory quotient (RQ) in eight parallel shake flasks [2]. Airflow of 10 NmL min^{-1} per flasks, which is equal to the ventilation conditions in shake flasks sealed with a cotton plug [3], was adjusted with a thermal mass flow controller. Oxygen partial pressure and differential gas pressure were measured via sensors located in the headspace of each flask, enabling the calculation of OTR, CTR and RQ [4]. Commercial versions of RAMOS are available from Kühner (Birsfelden, Switzerland) and Hitech Zang (Herzogenrath, Germany). For studying and characterizing microbial systems and optimizing the medium, this device has already been intensively used [32, 39, 44]. The experiments in this study were conducted at least twice, often up to four times and showed a good reproducibility with deviations of maximum 5 %.

Sampling and offline analysis

Multiple main cultivations—under identical culture conditions as for the RAMOS device—were performed in parallel in non-baffled 250 mL-shake flasks. For offline analysis, one shake flask of a parallel identical cultivation was removed from the shaking tray at each sampling time point and was not used for culturing thereafter. The taken samples were used to measure the optical density (OD_{600}), pH-value, osmolality, glucose and products (GA, 2KGA, 5KGA, acetate).

The OD_{600} of the cell broth was determined with a Genesys 20 photometer (Thermo Scientific, Dreieich, Germany) in semi-micro cuvettes (PS, Carl Roth, Karlsruhe, Germany) with 1 mL filling volume. Since $CaCO_3$ is

almost insoluble in water, it had to be removed by adding acetic acid (15 % w/v) prior to OD_{600} measurement.

For the analysis of pH, osmolality, glucose and products (GA, 2KGA, 5KGA, acetate) in the supernatant, a sample volume of 1 mL was transferred into a 1.5 mL Eppendorf tube and centrifuged for 5 min at 10,000×g. The pH-value was measured with a pH 510 probe (Eutech Instruments, Nijkerk, Netherlands) and the osmolality with an Osmomat 030 (Gonotek, Berlin, Germany). Glucose concentrations were quantified via an enzymatic assay (Boehringer Mannheim, Germany). The assay procedure was adapted to a 96-well microtiter plate using only 10 % of the volumes, compared to what is specified by the manufacturer, reaching a target volume of 300 µL. Absorbance at 340 nm was measured in a Synergy 4 plate reader (BioTek Instruments, Bad Friedrichshall, Germany). For product analysis, the supernatant was diluted with deionized water (1:4) and filtrated through a 0.2 µm PVDF filter (Carl Roth, Karlsruhe, Germany). Concentrations of gluconic acid (GA), 2-keto-gluconic acid (2KGA), 5-keto-gluconic acid (5KGA) and acetate (HAc) were determined via HPLC. The different metabolites were quantified using an organic acid resin column (250 × 8) including a pre-column (CS-Chromatographie Service, Langerwehe, Germany) at 80 °C. 1 mM H_2SO_4 was used as eluent at a flow rate of 0.8 mL min^{-1}. The sample volume was 20 µL.

Calculation of osmolality, water activity and osmotic pressure

To quantify the total osmolality of the differently buffered main cultivation media, the osmolality of the basic complex medium was measured. Then, the increase in osmolality caused by the buffering agents in its different dissociation states was mathematically added according to the following calculation. The dissociation of a buffer in aqueous solution can be described by the following equilibrium:

$$A^- + H^+ \rightleftarrows HA \tag{1}$$

where A^- denotes the dissociated form and HA, the undissociated form. The respective concentrations are given as:

$$[HA] + [A^-] = [HA + A^-]. \tag{2}$$

Hereby, $[HA + A^-]$ corresponds to the total applied buffer concentration of 0.22 mol L^{-1}. Assuming that pH buffering follows the equation of Henderson and Hasselbalch (Eq. 3) [33]

$$pH(t) = pK_a - \log \frac{[HA](t)}{[A^-](t)}, \tag{3}$$

The concentration of the different dissociation forms of the buffer can be obtained by inserting Eq. (2) into Eq. (3) and rearranging to

$$[HA] = \frac{[HA + A^-] \times 10^{(pK_a - pH)}}{1 + 10^{(pK_a - pH)}} \tag{4}$$

and

$$[A^-] = \frac{[HA + A^-]}{1 + 10^{(pK_a - pH)}} \tag{5}$$

For each deprotonized molecule, one proton remains in the medium (Eq. 6)

$$[A^-] = [H^+] \tag{6}$$

The respective pK_a value of the respective buffer at 30 °C (see Table 1), the initial pH-value of 6 and the total buffer concentration $[HA + A^-]$ were inserted in Eqs. (4) and (5), and the initial osmolalities of the applied buffers were calculated as follows:

$$\text{Osmolality}_{\text{initial}} = \text{Osmolality}_{\text{base medium,measured}} + \frac{[H^+] + [A^-] + [HA]}{\rho_{\text{medium}}} \tag{7}$$

where ρ_{medium} denotes the density of the fermentation medium assumed to be 1 kg L^{-1}.

Water activities a_W were calculated from measured osmolalities c_T (osmol kg^{-1}) and molal water concentration c_W (55.51 mol kg^{-1}) as follows:

$$a_W = \frac{1}{1 + \frac{c_T}{c_W}}[-]. \tag{8}$$

Instead of water activity a_W, the term "osmotic pressure" π is frequently used in literature. Osmotic pressure and water activity can be converted into each other with the following equation [18, 29]:

$$\pi = \frac{-RT \ln a_W}{V_W}[\text{bar}] \tag{9}$$

with the gas constant R (8.314×10^{-5} m^3 bar mol^{-1} K^{-1}), the temperature T (303 K) and the partial molal volume of water V_W (1.8×10^{-5} m^3 mol^{-1}).

The Davey model

In 1989, Davey et al. [10] reported a model which describes the influence of water activity on the microbial growth:

$$\ln \mu_{\max} = C_0 + \frac{C_1}{T} + \frac{C_2}{T^2} + C_3 a_w + C_4 a_w^2 \tag{10}$$

In this study, the Davey model was converted to the following form for constant temperature T:

$$\mu_{\max} = \mu_m \cdot e^{-\frac{1}{2}\left(\frac{a_{w,m} - a_w}{d a_w}\right)^2} \tag{11}$$

with

$$a_{w,m} = \frac{-C_3 \cdot C_4}{2}, \tag{12}$$

$$\mu_m = e^{\left(C_0 + \frac{C_1}{T} + \frac{C_2}{T^2} - \frac{C_3^2 \cdot C_4}{4}\right)}, \tag{13}$$

and

$$da_w = \frac{-C_3 - \sqrt{-2 \cdot C_4} \cdot C_4}{2} - a_{w,m} \tag{14}$$

where μ_m denotes the maximal growth rate at the optimal water activity $a_{w,m}$. The parameter da_w describes the width of the fit curve. Equation (11) is easier to use than Eq. (10), because all parameters in Eq. (11) have physiochemical meanings.

Results and discussion

Buffer screening

Cultivations of *G. oxydans* ATCC 621H and DSM 3504 were characterized and compared in unbuffered systems, $CaCO_3$-buffered systems (reference), and the systems with soluble buffers. Important parameters, such as pH-value and optical density at the end of the fermentation were evaluated.

Depending on the applied buffer, cultivations of both *G. oxydans* strains showed significant differences in the oxygen transfer rate (OTR), total oxygen consumption, final OD_{600} and pH-value (Fig. 1; Table 2). As Fig. 1a illustrates, the OTR curves of unbuffered, $CaCO_3$-, MES- and PIPPS-buffered cultivations for the ATCC 621H strain increase exponentially until a maximum OTR value is reached after about 5.5 h which implies non-limited exponential growth. At this time points the maximum OTR values are 35 mmol L^{-1} h^{-1} (unbuffered), 45 mmol L^{-1} h^{-1} ($CaCO_3$), 49 mmol L^{-1} h^{-1} (MES) and 46 mmol L^{-1} h^{-1} (PIPPS). This time point of 5.5 h indicates a low residual glucose concentration which is attributed to oxidation of glucose to GA during the exponential growth phase (Figs. 2c, d, 3d, e).

After reaching the maximum OTR-value the curve for the unbuffered cultivation of strain ATCC 621H drops down to zero (Fig. 1a). This can be explained by the low final pH-value of 2.58 (Table 2) that inhibits bacterial growth and metabolism. Accordingly, the final OD_{600} of 2.11 was low (Table 2). Even though *G. oxydans* can generally grow at a pH-value as low as 2.5, the enzymes of the PPP are inhibited at pH-values below 3.5. This inactivated PPP leads to low productivity and a poor cell yield [30]. Since the pH-value during the cultivation is clearly below the optimal pH-value of 6 for D-gluconate dehydrogenase [26, 42], GA is not oxidized to 2KGA. This is indicated by the completely ceased respiration activity after GA formation at 5.5 h (Figs. 1a, 2c), which implies that there is no diauxic growth on a second substrate. In comparison to the buffered cultivations, the osmolality of 0.317 osmol kg^{-1} for the unbuffered medium is relatively low (Table 2). Therefore, the low pH-value and not the osmolality causes for inhibited growth and respiration activity of strain ATCC 621H in unbuffered media (Fig. 1a).

With the reference buffer $CaCO_3$, the final pH-value of the strain ATCC 621H of 6.37 was slightly higher than the initial pH-value of 6 (Table 2). A final OD_{600} of 5.83 was obtained (Table 2) which is likely overestimated due to remaining particles, though, pretreated with acetic acid. After the maximum was reached at 5.5 h, the OTR curve decreases to around 18 mmol L^{-1} h^{-1} (Fig. 1a). Subsequently, the OTR increases and stays constant at about 22 mmol L^{-1} h^{-1} between 6 and 14 h. Afterwards, it decreases to zero at about 22 h, thereby indicating a clear diauxic growth phase on GA (Fig. 2f). As revealed by Fig. 2d, GA is oxidized to 2KGA and 5KGA in this second oxidation phase. This diauxic growth shows that the pH-value of around 6 (Fig. 2f) is optimal for the GA dehydrogenase [26, 42]. Detailed information about the $CaCO_3$ buffered cultivation is given in the next section.

Using the soluble MES buffer, the OTR curve of strain ATCC 621H reaches a higher maximum at 5.5 h than that of the unbuffered cultivation (Fig. 1a), but then rapidly falls to zero like the unbuffered cultivation. There is no second oxidation phase. These results are supported by the final OD_{600} and pH-value (Table 2). The OD_{600} value of 1.88 was even lower than that for of the unbuffered fermentation. The pH-value of 3.25 indicates that only insufficient buffering occured. Here, the pH-value could not be kept in the optimal range for *G. oxydans* of between 5.5 and 6 [20] although the pK_a value of MES is 6.1 at 30 °C (Table 1). Even though it was expected that MES would be a good buffer, it was not. Reduced growth and product formation is presumably caused by the significantly higher osmolality of the MES-buffered medium than that of the $CaCO_3$-buffered systems (Table 2).

Respiration activities of MES- and PIPPS-buffered cultivations during the first oxidation phase until 5.5 h were identical (Fig. 1a). In contrast to the OTR curve of the MES-buffered cultivation, the curve for the PIPPS-buffered cultivation does not drop to zero after glucose depletion (Figs. 1a, 3b, e). The OTR value decreases rapidly to a level of about 10 mmol L^{-1} h^{-1} at 6 h and subsequently slowly to zero until 30 h, thereby indicating a weak second oxidation phase. Again, GA is oxidized to 2KGA and 5KGA during this second oxidation phase (Fig. 3e). Biomass formation is almost equal to that of the unbuffered cultivation

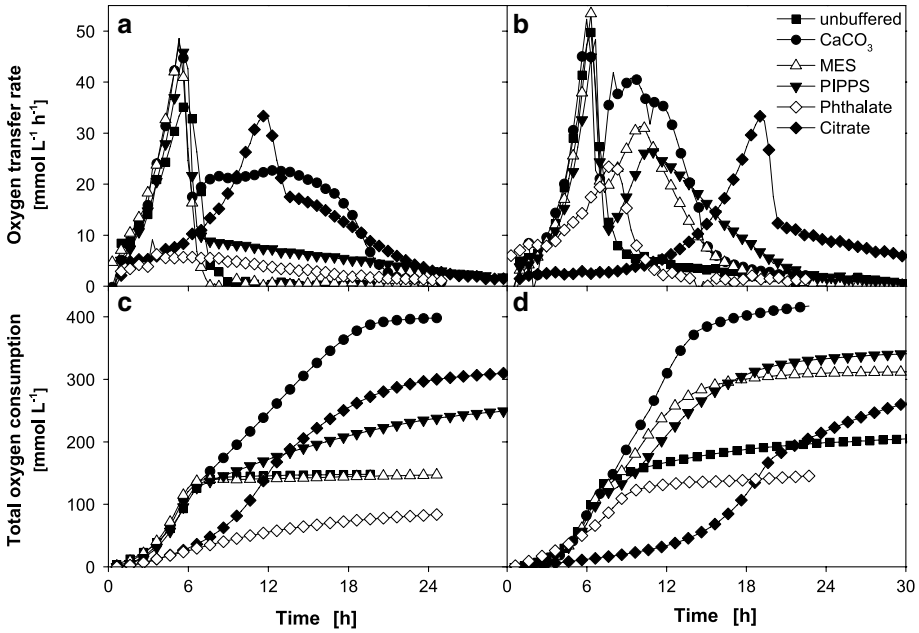

Fig. 1 Oxygen transfer rate and total oxygen consumption during the growth of *Gluconobacter oxydans* ATCC 621H (**a**, **c**) and DSM 3504 (**b**, **d**) in complex glucose medium (main ingredients: 40 g L^{-1} glucose, 5 g L^{-1} yeast extract) with different buffer systems (0.22 mol L^{-1}). Cultivation conditions: 30 °C, initial pH 6, 250 mL non-baffled shake flasks with 10 mL filling volume, 350 rpm shaking frequency, 50 mm shaking diameter

Table 2 Comparison of optical densities (OD_{600}) and pH-values at the end of fermentations in complex medium with 0.22 M glucose with and without utilization of different buffer (0.22 M) components[a]

Buffer component	*G. oxydans* ATCC 621H		*G. oxydans* DSM 3504		Initial osmolality measured (osmol kg^{-1})	Initial osmolality calculated (osmol kg^{-1})[c]
	$OD_{600,end}$ [−]	pH_{end} [−]	$OD_{600,end}$ [−]	pH_{end} [−]		
unbuffered	2.11	2.58	2.78	2.29	0.317 ± 0.008	–
$CaCO_3$	5.83[b]	6.37	Not measured	5.29	0.328	0.317
MES	1.88	3.25	5.38	2.71	0.654	0.624
PIPPS	2.16	3.7	3.3	3.48	0.763	0.739
DEPP	1.09	3.96	2.4	3.9	0.718	0.734
Phthalate	1.24	4.41	2.53	4.38	0.938	0.958
Citrate	2.63	4.79	–	–	0.962	1.027

[a] Mean values of duplicate cultures are shown. The duplicates differ less than 5 %

[b] Remaining carbonate was removed by adding acetic acid (15 % w/v)

[c] Osmolalities were calculated using Eq. (3)

(PIPPS: $OD_{600,end}$ = 2.16, unbuffered: $OD_{600,end}$ = 2.11) (Table 2). The pH-value decreases to 3.7, indicating a better buffer performance of PIPPS than MES, even though in terms of the relevant pK_a values (Table 1) of 3.72 and 6.1 for PIPPS and MES, respectively, PIPPS should have been less suitable as a buffer than MES. The PIPPS-buffered cultivation shows higher 2KGA, 5KGA and biomass formation (Fig. 3e, h), than the cultivation with MES buffer (Fig. 3d, g). Moreover, the higher osmolality of PIPPS (0.763 osmol kg^{-1}) compared to that of MES-buffered medium (Table 2) points to higher osmotic stress for the bacteria. This, in turn, leads to the assumption that the use of PIPPS would reduce growth and productivity. However, the acquired data reveal the opposite.

In contrast to $CaCO_3$-, MES- and PIPPS-buffered cultivations, the cultivations with citrate showed a considerably different respiration behavior (Fig. 1a). A longer lag phase, followed by an exponential increase in the OTR (app. 3–12 h) can be observed. A maximum OTR value of 33 mmol L^{-1} h^{-1} is reached at 12 h. After glucose depletion (12 h), the OTR curve drops to a value of 18 mmol L^{-1} h^{-1} similar to the $CaCO_3$-buffered cultivation (Figs. 1a, 2b, d, 3c, f). Subsequently, a second oxidation phase occurs, characterized by the further oxidation of GA to 2KGA and 5KGA (Fig. 3c, f). Using citrate as buffer, a final OD_{600} of 2.63 (Table 2) was obtained. Consequently, the biomass formation was 25 % higher than that of the unbuffered cultivation. The pH-value at the end of the

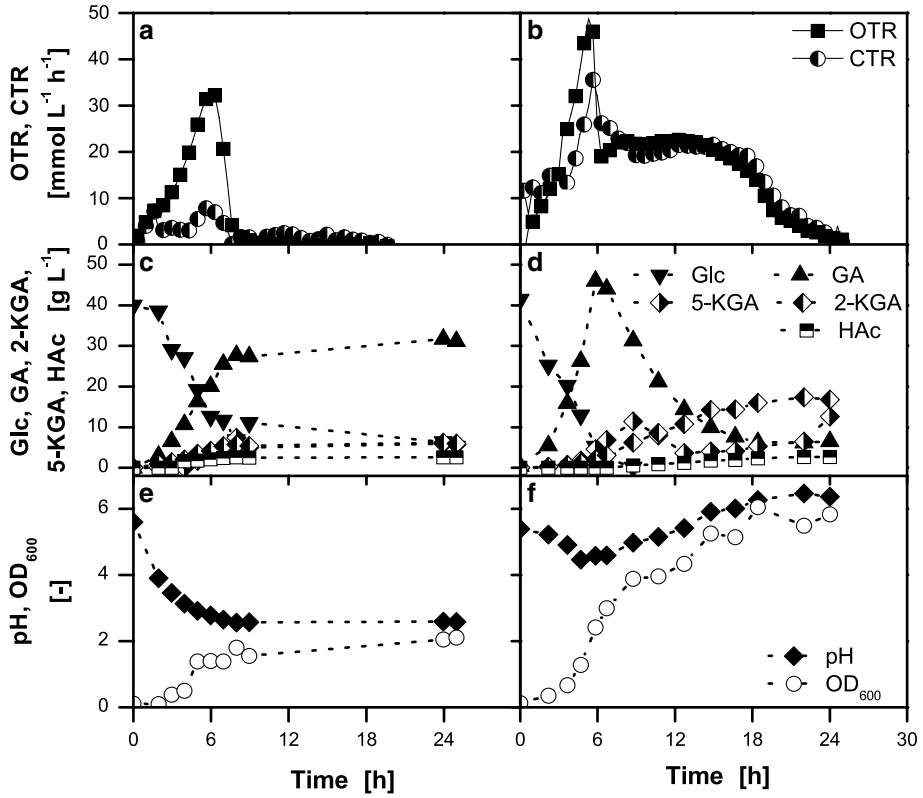

Fig. 2 Unbuffered (**a**, **c**, **e**) and $CaCO_3$ buffered (**b**, **d**, **f**) culture of *G. oxydans* ATCC 621H in complex glucose medium (main ingredients: 40 g L^{-1} glucose, 5 g L^{-1} yeast extract). Cultivation conditions: 30 °C, initial pH 6, 250 mL non-baffled shake flasks with 10 mL filling volume, 350 rpm shaking frequency, 50 mm shaking diameter

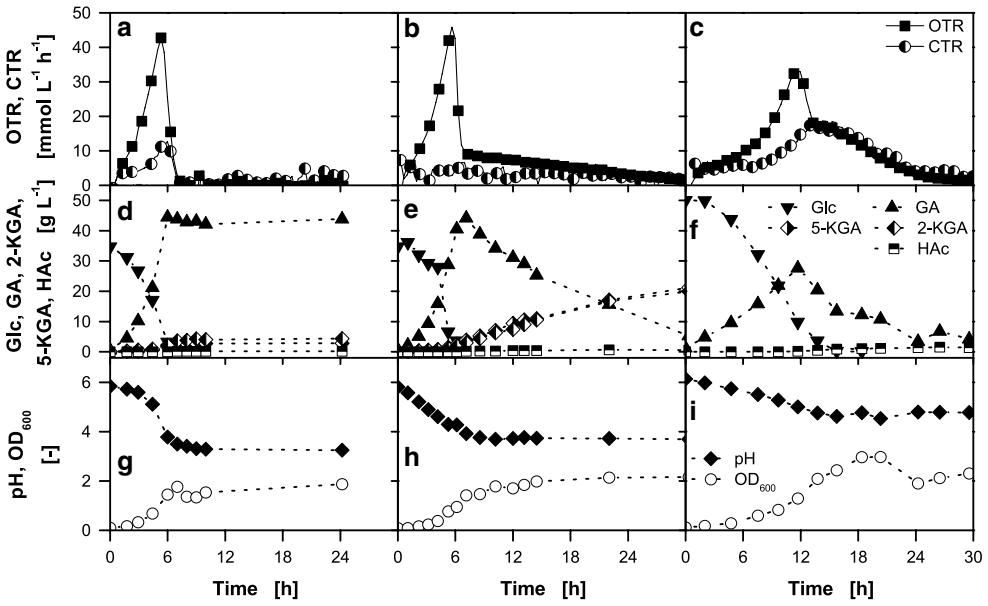

Fig. 3 MES (**a**, **d**, **g**), PIPPS (**b**, **e**, **h**) and citrate (**c**, **f**, **i**) buffered culture of *G. oxydans* ATCC 621H in complex glucose medium (main ingredients: 40 g L^{-1} glucose, 5 g L^{-1} yeast extract). Cultivation conditions: 30 °C, initial pH 6, 250 mL non-baffled shake flasks with 10 mL filling volume, 350 rpm shaking frequency, 50 mm shaking diameter

fermentation reached 4.79 (Table 2), which is close to the optimal range for growth and production. Consequently, the buffer performance of citrate is the best compared to the other soluble buffers. Nevertheless, the growth and respiration activity are clearly time-delayed. This time-delay, presumably indicating an inhibition, may be caused by the high osmolality of 0.962 osmol kg^{-1} in citrate containing medium (Table 2). A more detailed description of the observed respiration behavior and the underlying metabolism for MES, PIPPS and citrate-buffered cultivations of *G. oxydans* ATCC 621H will be given below.

It is noteworthy that no exponential growth for *G. oxydans* ATCC 621H (Fig. 1a) is observed in the phthalate-buffered system and the final OD_{600} is low (1.24, Table 2).

A maximum OTR-value of only 6 mmol L^{-1} h^{-1} is reached. Even though, the final pH-value of 4.41 (Table 2) is relatively high, the offline measurements indicate a very low GA formation (data not shown). Further analyses of the phthalate-buffered medium revealed a high osmotic stress (osmolality = 0.938 osmol kg^{-1}), thus, indicating inhibited bacterial growth and productivity. It has to be concluded that phthalate is not a good buffer for *Gluconobacter* species.

For unknown reason, the respiration activity for DEPP-buffered cultivations was found to be very low (data not shown) although the physiochemical parameters of the DEPP buffer are very similar to those of PIPPS. The measured osmolality was 0.718 osmol kg^{-1} and, thus, in the range of PIPPS. In addition, the pK_a value for DEPP (4.46) is more suitable for the desired pH-range between 4 and 6 than the pK_a for PIPPS (3.72) (Table 1). According to its insufficient performance, DEPP was not further investigated.

All aforementioned buffers were also tested for the cultivation of *G. oxydans* DSM 3504 (Fig. 1b). The OTR curves of unbuffered, $CaCO_3$-, MES- and PIPPS-buffered cultivations of the DSM 3504 strain increase exponentially until a maximum OTR-value is reached at 6 h (Fig. 1b). This implies an unlimited exponential growth of this strain. Maximum OTR-values of 50 mmol L^{-1} h^{-1} (unbuffered), 52 mmol L^{-1} h^{-1} ($CaCO_3$), 53 mmol L^{-1} h^{-1} (MES), and 48 mmol L^{-1} h^{-1} (PIPPS) are observed. The citrate-buffered cultivation of DSM 3405 is time-delayed compared to strain ATCC 621H and attains its maximum OTR value after 18 h (Fig. 1b).

In contrast to strain ATCC 621H (Fig. 1a), the OTR curve of the unbuffered cultivation of strain DSM 3504 (Fig. 1b) does not decrease to zero after the OTR maximum is reached at 6 h. Instead, the OTR curve plummets to a value of around 5 mmol L^{-1} h^{-1} and then steadily decreases to zero at 30 h indicating a weak, prolonged second oxidation phase of GA. Thus, strain DSM 3504 seems to be more acid-tolerant than strain ATCC 621H. This is supported by a lower final pH-value of 2.29 measured for the unbuffered cultivation of strain DSM 3504 compared to a final pH-value of 2.58 for the unbuffered cultivation of strain ATCC 621H (Table 2). A significant second oxidation phase can also be observed for $CaCO_3$-, MES-, PIPPS- and citrate-buffered cultivation of DSM 3504. In comparison to strain ATCC 621H, the second oxidation phases in $CaCO_3$-, PIPPS- and citrate-buffered cultivations of strain DSM 3504 (Fig. 1a, b) were more pronounced, as indicated by the higher OTR signals (Fig. 1b). With respect to the second oxidation phase of the MES-buffered system, both strains of *G. oxydans* differ strongly from one another. Strain DSM 3504 depicts a sharp second oxidation phase unlike that of ATCC 621H which was completely missing. Compared to strain ATCC 621H, the respiration activity of the phthalate-buffered cultivation of strain DSM 3504 is increased as well. However, the phthalate buffer is not as effective as the other tested buffers, since respiration is inhibited and a maximum OTR value of only 23 mmol L^{-1} h^{-1} is obtained (Fig. 1b).

In general, strain DSM 3504 has a higher biomass formation and productivity than the strain ATCC 621H, which is indicated by the altogether higher respiration activities (Fig. 1a, b), higher final OD_{600}-values and lower final pH-values (Table 2). Therefore, the tolerance of strain DSM 3504 to soluble buffers is higher than that of strain ATCC 621H. Since the OTRs of both *G. oxydans* strains were highest in $CaCO_3$-buffered cultivations, this buffer was the most suitable one. Using the OTR signals measured in the respective exponential phases up to 6 h, the specific maximum growth rates for both strains were calculated. Interestingly, *G. oxydans* DSM 3504 grew slower (0.49 h^{-1}) than *G. oxydans* ATCC 621H (0.6 h^{-1}).

The integral under the OTR curve depicts the total oxygen consumption during cultivation and is illustrated in Fig. 1c, d. Glucose oxidation can be stoichiometrically evaluated by means of the total oxygen consumption. For each oxidation step, the required amount of oxygen is 0.5 mol O_2 per mol of oxidized compound. Taking into account the initial glucose concentration of 222 mmol L^{-1} the required oxygen amount for 100 % D–gluconate formation is 111 and 222 mmol L^{-1} for the two aforementioned keto-gluconates, respectively. The total measured oxygen consumption of about 120 mmol L^{-1} at 6 h for cultivations of both strains with $CaCO_3$, MES, and PIPPS reveals that glucose is completely oxidized to GA. The excess of ca. 10 mmol L^{-1} measured oxygen consumption presumably originated from biomass formation on yeast extract.

Taking the total oxygen consumption at the end of fermentation as a measure for productivity, it becomes clear, that the $CaCO_3$-buffered systems (ATCC 621H: 399 mmol L^{-1}; DSM 3504: 415 mmol L^{-1}) have the highest biomass formation and the highest amount of oxidation products. For strain ATCC 621H, citrate (309 mmol L^{-1}) or PIPPS (249 mmol L^{-1}) can be a feasible buffer alternative to $CaCO_3$. Moreover, in the cultivations of strain DSM 3504, PIPPS (340 mmol L^{-1}) or MES (312 mmol L^{-1}) are viable options. Nevertheless, $CaCO_3$ is the best buffer system in terms of biomass formation and oxygen consumption. The main reason for this phenomenon might be that $CaCO_3$ remains in the solid state in the absence of acids. Thus, with $CaCO_3$, the osmotic pressure acting on the microorganisms remains constantly low. By contrast, soluble buffers increase the osmolality and, therefore, the osmotic pressure which might adversely affect the microorganisms. Thus, osmolalities of the cultivation media were measured and calculated (Table 2). The calculated

osmolalities are in good agreement with the empirical values. Since osmolalities remained nearly constant during the fermentations (data not shown), the measured initial osmolalities were assumed to be constant for the whole cultivation: By adding soluble buffers the osmolalities of the media increased by 100–200 % compared to those of the unbuffered or $CaCO_3$-buffered media. The influence of higher osmolalities on *G. oxydans* will be discussed in detail below.

Comparison of unbuffered and $CaCO_3$-buffered cultivation of *G. oxydans* ATCC 621H

To gain a better understanding of the occurring phenomena during cultivation of *G. oxydans* ATCC 621H with the investigated buffer systems, offline samples were taken during cultivation and analyzed with respect to metabolite concentrations, pH-, and OD_{600}-values. The results for unbuffered and $CaCO_3$-buffered (reference buffer) fermentations of *G. oxydans* 621H are illustrated in Fig. 2. The courses of OTR and CTR curves of unbuffered cultivation (Fig. 2a) reveal a strong oxidation phase during the first 6 h of cultivation, since the CTR is significantly lower than the OTR. At this time point, the pH-value drops below 3 (Fig. 2e), thereby stopping the oxidation processes as well as biomass formation. Only a small amount of the generated GA was oxidized to keto-gluconates (Fig. 2c). Metabolite formation yielded 31 g L^{-1} GA, 6 g L^{-1} 2KGA, 6 g L^{-1} 5KGA and 2.5 g L^{-1} acetate (HAc), while 6 g L^{-1} D-glucose remained unoxidized.

Throughout the whole $CaCO_3$-buffered cultivation the OTR and CTR level was clearly higher (Fig. 2b) than for the unbuffered one (Fig. 2a), revealing a higher respiration activity and productivity. The pH-value of the $CaCO_3$-buffered cultivation decreased only to 4.5 within 5 h before rising again to a final pH-value of 6.37 (Fig. 2f). This pH-range offers highly improved bacterial growth conditions in comparison to the unbuffered cultivation. At 5 h, the maximum OTR of 49 mmol L^{-1} h^{-1} is reached, indicating glucose depletion due to its complete oxidation to GA (Fig. 2d) and biomass formation (Fig. 2f). The strikingly high CTR in the $CaCO_3$-buffered system (Fig. 2b) is caused by the release of CO_2 from the buffer. In the presence of acids, the buffer $CaCO_3$ partly dissociates to Ca^{2+} and carbonic acid resulting in CO_2 which gasses out. Consequently, the illustrated CTR curve in Fig. 2b shows a mixture of acid formation and respiration activity. After 5 h, the pH-value slightly increases, while GA is consumed, indicated by its decreasing concentration from 45 to 6 g L^{-1} (Fig. 2d). Within this second oxidation phase (5–24 h), 16.8 g L^{-1} 2KGA, 12.6 g L^{-1} 5KGA and 2.7 g L^{-1} HAc are formed. Ultimately, the cultivation of *G. oxydans* ATCC 621H in $CaCO_3$-buffered medium allows for higher biomass and product formation compared to the unbuffered cultivation.

Cultivation of sp. *G. oxydans* ATCC 621H in soluble buffers MES, PIPPS and citrate

As mentioned before, the respiration activity of *G. oxydans* 621H depends on the applied soluble buffer (compare Fig. 3a–c). During cultivations with MES, PIPPS and citrate buffers, D-glucose is completely oxidized after 6 h (MES and PIPPS) and 16 h (citrate) (Fig. 3d–f). The final pH-values were found to be 3.25 (MES), 3.7 (PIPPS) and 4.78 (citrate) at the end of the respective time points of 6 and 16 h. These values remained constant until the end of fermentations (Fig. 3g–i). It is hypothesized that the different respiration activities are attributed to the different pH profiles. The existence and length of the second oxidation phase correlates with the final pH-value. For cultivation with MES the lowest pH-value was measured and no second oxidation phase could be detected (Fig. 3a), whereas PIPPS- and citrate-buffered cultivations showed higher pH-values and a second oxidation phase (Fig. 3b, c).

In the MES-buffered culture, GA was only barely further oxidized which is in good agreement with the OTR curve dropping to zero after glucose depletion (Fig. 3a, d). Consequently, the GA concentration of 44 g L^{-1} stays constant and only small amounts of keto-gluconates (4.35 g L^{-1} 2KGA, 2.79 g L^{-1} 5KGA) are formed (Fig. 3d). Moreover, 0.17 g L^{-1} acetate was produced. The pH-value decreased below 3.5 (Fig. 3g), resulting in an inhibited PPP and leading to low biomass formation similar to that of the unbuffered cultivation (Fig. 2e).

On PIPPS-buffered medium (Fig. 3b, e, h), *G. oxydans* 621H further oxidized GA from a concentration of 44 g L^{-1} to a final concentration of 5.19 g L^{-1} after 30 h. Accordingly, compared to the MES-buffered cultivation, the production of 5KGA and 2KGA was more than 7-fold (21.17 g L^{-1}) and 4-fold (19.94 g L^{-1}), respectively. The oxidation of GA to 2KGA and 5KGA (Fig. 3e) in the second oxidation phase is also visible in the consistent decline of the OTR curve from ca. 10 mmol L^{-1} h^{-1} at 6 h to zero at 30 h (Fig. 3b). Acetate in a concentration of 0.6 g L^{-1} was formed (Fig. 3e), which is 24 % compared to that of the unbuffered fermentation (Fig. 2c). Biomass formation in PIPPS-buffered cultivation ($OD_{600} = 2.16$) was almost equal to that of the unbuffered cultivation ($OD_{600} = 2.11$) (Figs. 2e, 3h; Table 2).

As mentioned before, the citrate-buffered *G. oxydans* ATCC 621H cultivation showed a time delay in respiration activity. A slightly higher OD_{600} of 2.31 is reached in comparison to the PIPPS- and MES-buffered systems (Fig. 3g–i, respectively). Almost no acetate was formed during the citrate-buffered growth. Gluconic

acid is oxidized to a residual amount of 4.19 g L^{-1} (21 mmol L^{-1}) (Fig. 3f), indicating the formation of keto-gluconates. Since the citrate peak in HPLC analysis overlapped those for keto-gluconates, these concentrations could not be measured. The keto-gluconate formation becomes particularly clear when considering the molar oxygen balance (Fig. 1c). The total oxygen consumption for citrate-buffered cultivation is 310 mmol L^{-1} (Fig. 1c). If one disregards cell growth, the complete oxidation of 222 mmol L^{-1} glucose to an equimolar concentration of GA would in theory yield a total oxygen consumption of 111 mmol L^{-1}. Given the fact that 21 mmol L^{-1} GA remained unoxidized, only 201 mmol L^{-1} of GA were converted by *G. oxydans*. This would theoretically yield a total oxygen consumption of 100 mmol L^{-1}. Therefore, the oxidation of glucose to keto-gluconates requires a total oxygen consumption of 211 mmol L^{-1}. A dry cell weight of 0.62 g L^{-1} was derived from the final OD_{600} value of 2.31 and the empirical correlation according to a previous work of Richhardt et al. [37]. The respective molar cell concentration of *G. oxydans* 621H cells was calculated from the formula $C_5H_{8.9}NO_{1.9}$ [31]; it can be estimated from this that 10 mmol L^{-1} O_2 was needed for biomass formation. Consequently, only 221 mmol L^{-1} oxygen consumption are stoichiometrically explainable, while around 100 mmol L^{-1} consumed oxygen cannot be explained by direct oxidation of glucose, GA and by biomass formation. Most likely, citrate was used as an additional substrate in the incomplete citrate cycle which is indicated by the conspicuously high CTR values (max. 18 mmol L^{-1} h^{-1}) (Fig. 3c). In *G. oxydans,* CO_2 is usually formed by four metabolic steps: in the PPP during decarboxylation of 6-phosphogluconate to ribulose-5-posphate, at the end of the Entner–Doudoroff pathway during conversion of pyruvate to acetaldehyde or Acetyl-CoA, and in the incomplete citrate cycle during conversion of isocitrate to 2-oxoglutarate, and decarboxylation of 2-oxoglutarate and glutamine to succinyl-CoA. The citrate cycle in *G. oxydans* is incomplete, since it lacks the succinate dehydrogenase and the succinyl-CoA-synthase [17, 31, 43]. Thus, adding citrate apparently led to an enhanced activity of the incomplete citrate cycle and the release of 2 moles of CO_2 per mole of citrate. The formed CO_2 gassed out and resulted in the increase in the CTR values (Fig. 3c). NADH that was additionally formed in the incomplete citrate cycle was oxidized in the respiratory chain, causing the 100 mmol L^{-1} excess in oxygen consumption. This is illustrated by the equal CTR and OTR in the cultivation phase after 13 h (Fig. 3c). Since citrate is obviously not inert, this buffer was not further investigated.

To summarize, cultivations buffered with soluble components showed significantly less formation of biomass and product as well as lower respiration activity compared to the reference system with $CaCO_3$ buffer. Two major reasons for this phenomenon could be identified: (1) the pH-value could not be stabilized in the optimal range of 5.5–6, and (2) osmolality strongly increased because of the higher amounts of soluble buffer compounds. To understand the superior performance of $CaCO_3$ as a buffer, the pK_a and pH-values have to be taken into account to determine and evaluate the osmotic pressure.

Determination of osmotic sensitivity by addition of salts to $CaCO_3$-buffered cultivations

To investigate the influence of the osmotic pressure on *G. oxydans* 621H and DSM 3504, NaCl (Fig. 4), $MgSO_4$ (Fig. 5) or KCl (Online Resource 1) were added to the $CaCO_3$-buffered (0.22 mol L^{-1}) medium to achieve a defined increase of osmolality. Respiration activities were monitored using the RAMOS device.

In these experiments, NaCl concentrations were varied from 0 to 25 g L^{-1} resulting in osmolalities between 0.33 osmol kg^{-1} (plain medium) and 1.19 osmol kg^{-1} (Fig. 4). It could be observed that for both strains an increasing NaCl concentration leads to decreasing maximum OTR values (Fig. 4a, b). Furthermore, these OTR maxima were found to be shifted with time with increasing NaCl concentrations. The total oxygen consumed (Fig. 4c, d) until the maximum OTR was reached decreases as well. For the osmolality of 1.19 osmol kg^{-1} (25 g L^{-1} NaCl), no distinct OTR peak could be detected within the cultivation time (Fig. 4a, b). Consequently, the oxidation of D-glucose was slowed down and became more incomplete with increasing amounts of salts and, thus, at higher osmotic pressures.

Upon comparing the cultivations of strain ATCC 621H with that of DSM 3504, the decrease in the maximum OTR values was more pronounced for strain ATCC 621H (Fig. 4a, b). Thus, *G. oxydans* ATCC 621H reacts more sensitively to higher osmotic stress than *G. oxydans* DSM 3504. Increasing NaCl concentrations greatly affected the second oxidation phase (Fig. 4a, b). Already a NaCl concentration of 5 g L^{-1} led to a strong delay and decrease in the OTR curve for the second oxidation phase. For concentrations above 5 g L^{-1}, almost no second oxidation phase could be observed. The same phenomena were observed for both strains when adding KCl instead of NaCl (Online Resource 1).

Results for the variation of $MgSO_4$ concentration in the $CaCO_3$-buffered system are illustrated in Fig. 5. The concentration of $MgSO_4 \cdot 7\ H_2O$ was varied from 2.5 to 150 g L^{-1} (0.33–1.08 osmol kg^{-1}), thereby achieving osmolalities between 0.33 osmol kg^{-1} (plain medium) and 1.08 osmol kg^{-1}. Again, increasing salt concentrations and,

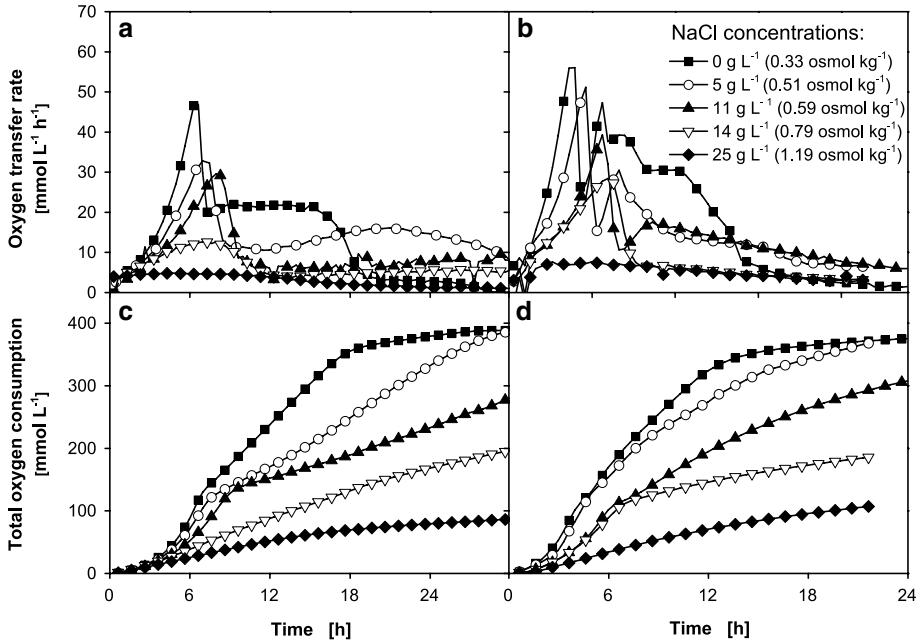

Fig. 4 Influence of the initial osmotic pressure on the oxygen transfer rate and on the total oxygen consumption during the growth of *Gluconobacter oxydans* ATCC 621H (**a**, **c**) and DSM 3504 (**b**, **d**) in complex glucose medium (main ingredients: 40 g L^{-1} glucose, 5 g L^{-1} yeast extract) with varying NaCl concentrations and $CaCO_3$ (0.22 mol L^{-1}). Cultivation conditions: 30 °C, 250 mL non-baffled shake flasks with 10 mL filling volume, 350 rpm shaking frequency, 50 mm shaking diameter

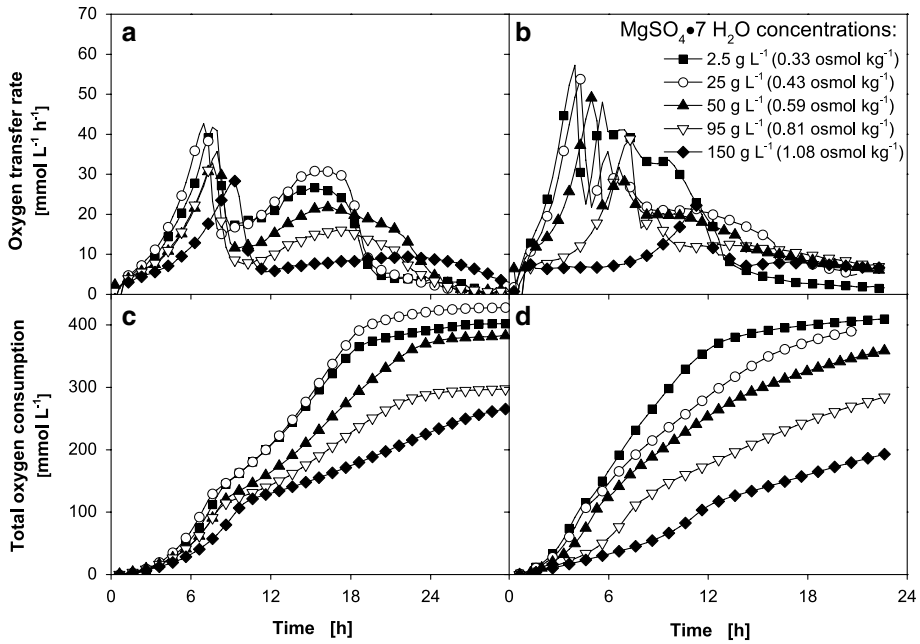

Fig. 5 Influence of the initial osmotic pressure on the oxygen transfer rate and on the total oxygen consumption during the growth of *Gluconobacter oxydans* ATCC 621H (**a**, **c**) and DSM 3504 (**b**, **d**) in complex glucose medium (main ingredients: 40 g L^{-1} glucose, 5 g L^{-1} yeast extract) with varying $MgSO_4$ (heptahydrate) concentrations and $CaCO_3$ (0.22 mol L^{-1}). Cultivation conditions: 30 °C, 250 mL non-baffled shake flasks with 10 mL filling volume, 350 rpm shaking frequency, 50 mm shaking diameter

thus, higher osmolalities result in delayed and decreased OTR maxima. Interestingly, with $MgSO_4 \cdot 7\ H_2O$ strain ATCC 621H seems to tolerate the increased osmolality better than strain DSM 3504. This is demonstrated by the comparably narrow time shift of the OTR maxima (Fig. 5a) and the distinct diauxic behavior even at higher osmolalities up to around 1 osmol kg^{-1} (150 g L^{-1} $MgSO_4 \cdot 7\ H_2O$) for strain ATCC 621H. In contrast, strain DSM 3504 shows more time-shifted OTR maxima and a diminished second oxidation phase (Fig. 5b). The differences between the two strains within the two oxidation phases become prominent when the total oxygen consumptions are compared to each other (Fig. 5c, d): *G. oxydans* ATCC 621H consumes about 120 mmol L^{-1} oxygen within the first 6–9 h of cultivation, whereas the strain DSM 3504 needs 5–12 h. This amount of 120 mmol L^{-1} consumed oxygen implies the total oxidation of D-glucose (222 mmol L^{-1}) to GA. Additionally, the slope of the curve of total oxygen consumption in the second oxidation phase of strain DSM 3504 is lower with increasing salt concentration (Fig. 5d), demonstrating a slower conversion of GA. Within 22 h, strain DSM 3504 could not completely oxidize the GA which is indicated

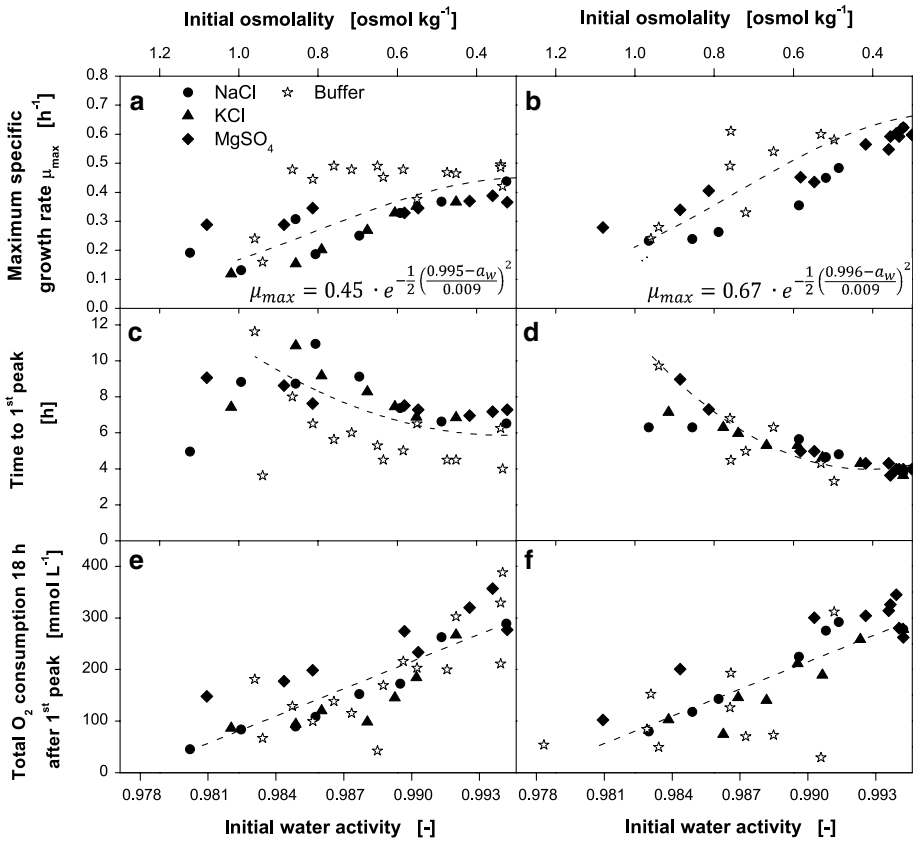

Fig. 6 Influence of the initial osmotic pressure or water activity on the maximum specific growth rate μ_{max}, time to the 1st OTR peak, and on the total oxygen consumption until 18 h after 1st OTR peak for *Gluconobacter oxydans* ATCC 621H (**a**, **c**, **e**) and DSM 3504 (**b**, **d**, **f**) in complex glucose medium (main ingredients: 40 g L^{-1} glucose, 5 g L^{-1} yeast extract) with $CaCO_3$ (0.22 mol L^{-1}). 30 °C, 250 mL non-baffled shake flasks with 10 mL filling volume, 350 rpm shaking frequency, 50 mm shaking diameter. The dashed lines symbolize fits according to the modified Davey model (Eq. 11) (**a**, **b**), quadratic polynomial (**c**, **d**) and linear (**e**, **f**) approximations and for data illustrated above. Quadratic polynomials are: ATCC 621H, $t_{\text{the first peak}} = 10.86\ a_w^2 - 7.04\ a_w + 7$ with $R^2 = 0.96$; DSM 3504. $t_{\text{the first peak}} = 20.96\ a_w^2 - 17.16\ a_w + 7.47$ with $R^2 = 0.54$. Linear approximations are: ATCC 621H, $O_{2,\text{consumed}} = -308.5\ a_w + 389.5$ with $R^2 = 0.62$; DSM 3504. $O_{2,\text{consumed}} = -308.1\ a_w + 388.7$ with $R^2 = 0.61$

by the still increasing oxygen consumption (Fig. 5d). By contrast, strain ATCC 621H totally converts GA within the same time at osmolalities of up to 0.8 osmol kg^{-1} (95 g L^{-1} $MgSO_4 \cdot 7\ H_2O$) (Fig. 5c).

By contrast with NaCl and KCl, $MgSO_4$ is not an inert salt, since its ion Mg^{2+} is known as a complexing ion for enzymes and, thus, enhances their activity [8, 12]. Consequently, the absence of $MgSO_4$ led to reduced respiration activity, exemplary investigated for the growth of strain DSM 3504 (data not shown).

Growth of *G. oxydans* as a function of water activity

Figure 6 summarizes the cultivations for buffer screening (see Figs. 1, 2, 3) and with varying salt concentrations (see Figs. 4, 5, and KCl) for both strains with respect to the initial osmolality and the corresponding water activity. The specific maximum growth rates μ_{max}, the times of the first OTR peak, and the total oxygen consumption until 18 h after the first OTR peak had been reached are depicted. As Figs. 4 and 5 show, the differences in the OTR curves are especially striking during the second oxidation phase, that means after the first OTR peak. Consequently, the oxygen consumption after reaching the first OTR peak was used as evaluation parameter. Since cultivations were stopped minimum 18 h after the first OTR peak, the same time period was chosen, enabling the direct comparison of both strains.

There are clear trends. Decreasing osmolality, thus increasing water activity, resulted in increasing maximum specific growth rates (μ_{max}), decreasing times until the first OTR peak was attained, and increasing total oxygen consumptions up to 18 h after the first OTR peak had been reached for *G. oxydans* ATCC 621H (Fig. 6a, c, e) and DSM 3504 (Fig. 6b, d, f). Maximum specific growth rates μ_{max} were fitted according to the modified Davey model (Eq. 11) as illustrated in Fig. 6a, b (dashed lines). The data

for the times until reaching the first peak of the OTR curve were approximated with a quadratic polynomial as illustrated in Fig. 6c, d. Water activities lower than 0.990 led to reduced growth rates and longer times until the first peak was attained. Data sets for total oxygen consumption until 18 h after the first peak could be linearly approximated (Fig. 6e, f, dashed lines). With decreasing water activities, the total oxygen consumption decreased, indicating that the oxidations of formed GA to 2KGA or 5KGA and the subsequent oxidation of 2KGA to DKGA in DSM 3504 were inhibited as well.

The results in Fig. 6a, c for the growth of *G. oxydans* ATCC 621H show, that the reduction of water activity by adding buffers, led to slightly higher maximal specific growth rates and shorter times until the first OTR peaks were reached, when compared to the salt variation experiments. One reason might be a higher toxicity of NaCl, KCl and $MgSO_4$ compared to the investigated buffers. This phenomenon should be investigated in a future study.

The results in Fig. 6 demonstrate a high osmotic sensitivity of *G. oxydans* ATCC 621H and DSM 3504. The considerably reduced growth characteristics at water activities of below 0.99 are in good agreement with the lower osmotic resistance of the bacteria in comparison to yeasts, for example. While yeasts can grow in media with water activities as low as 0.85, bacteria tolerate only water activities that are higher than 0.9 [7]. In 1976, Sterne et al. [46] investigated the influence of osmotic pressure on the growth of the fungi *Phytophthora cinnamomi* by variation of NaCl, KCl and $MgSO_4$ concentrations, amongst others. The experiments in this study were conducted with a water activity in the range of 0.995 (osmotic pressure in the range of 7 bar) to 0.98 (28 bar). Optimal growth of *P. cinnamomi* occurred at an osmotic pressure of 7 bar. Growth was reduced by 50 % at a water activity a_w of ca. 0.9935 (9 bar) adjusted with NaCl or KCl. If the osmotic pressure was adjusted with $MgSO_4$, growth of *P. cinnamomi* was already 50 % at $a_w = 0.997$ (4 bar). Interestingly, the two *G. oxydans* strains investigated here exhibited a higher osmotic tolerance than the fungi *P. cinnamomi*, which contradicts to Brown [7], who stated higher osmotic tolerances of fungi in comparison to bacteria. Sterne et al. stated that NaCl, KCl and $MgSO_4$ influence growth only by altering the osmotic pressure. In the current study, this could be confirmed for *G. oxydans*. Comparable results were obtained by Woods and Duniway [50] who showed the influence of osmotic pressure on *Phytophthora cryptogea* and *Fusarium moniliforme* when using NaCl, KCl and $MgSO_4$ to increase the osmotic pressure. Gao et al. [15] cited inhibitory effects on the growth of *G. oxydans* WSH-003 when osmotic pressure was increased due to high concentrations of 2-ketogulonic acid (>140 g L^{-1}). Furthermore, an early study by Mori et al. [28] reported the inhibitory effect of increasing osmotic pressure due to increased substrate concentrations during the cultivation of *G. xydans* ATCC 621H. Growth rate and product formation rate decreased as osmotic pressure increased, which is perfectly concordant with the results presented in this work. However, water activities were not mentioned in the latter two publications. Because of the membrane permeability to water and impermeability to most solutes, living cells are affected by changes in the total solute concentration in the surrounding medium, which inherently means a change in osmotic pressure. A detailed study regarding the responses of *Escherichia coli* (*E. coli*) to osmolarity in a range of 0.1–3 osmol L^{-1} was presented by Record et al. [36]. In this cited study, optimal growth rates were obtained at 0.28 osmol L^{-1}. To compare the results of our study with those of Record et al. it was assumed that the density of the medium is equal to that of water (1 kg L^{-1}). Thereby, the osmolarity (osmol L^{-1}) is equal to the osmolality (osmol kg^{-1}). The herein determined optimum osmolality for *G. oxydans* of approximately, 0.4 osmol kg^{-1} is slightly higher than the optimum for *E. coli* (0.28 osmol kg^{-1}). *Escherichia coli* reacts to increasing osmolarity (>1 osmol L^{-1}) by releasing free cytoplasmic water. Thus, the concentration of cytoplasmic solutes increases, resulting in strongly reduced growth of *E. coli*. After addition of the osmoprotectant glycerine betaine (1 mol L^{-1}), free cytoplasmic water was increased. Furthermore, the *E. coli* growth rate increased almost twofold. In further studies, the applicability of such an osmoprotectant for the cultivation of *G. oxydans* could be investigated.

In Fig. 7 the impact of water activity on normalized growth rate is shown for *G. oxydans* ATCC 621H and DSM 3504 in comparison to several other microorganisms. The plotted curves are fits according to the modified Davey model as given by Eq. (11). The corresponding fitting parameters are given in Table 3. As illustrated, the two investigated strains *G. oxydans* ATCC 621H and DSM 3504 possess a low-osmotic tolerance, when compared to other, mostly bacterial, strains. Only the fungi *Phytophtora cinnamomi* grown on minimal medium with NaCl as osmoticum [46] is more osmotic-sensitive than the two *G. oxydans* strains, even though these strains have the same optimum of the maximal specific growth rate at a water activity of 0.995. This is indicated by the stronger drop of the curve for the *P. cinnamomi* in comparison to the curves of *G. oxydans* 621H and DSM 3504. *Escherichia coli* grown on minimal medium with NaCl as osmoticum, as reported by Record et al. [36], is equally osmotic-sensitive, compared to both *G. oxydans* strains. By contrast, when *E. coli* was cultivated on rich medium, it showed an increased osmotic tolerance indicated by the decrease of the minimal water activity for growth from 0.973 to 0.95 (see Fig. 7). In 1978 Prior [34] described the dependency of the specific growth rates of

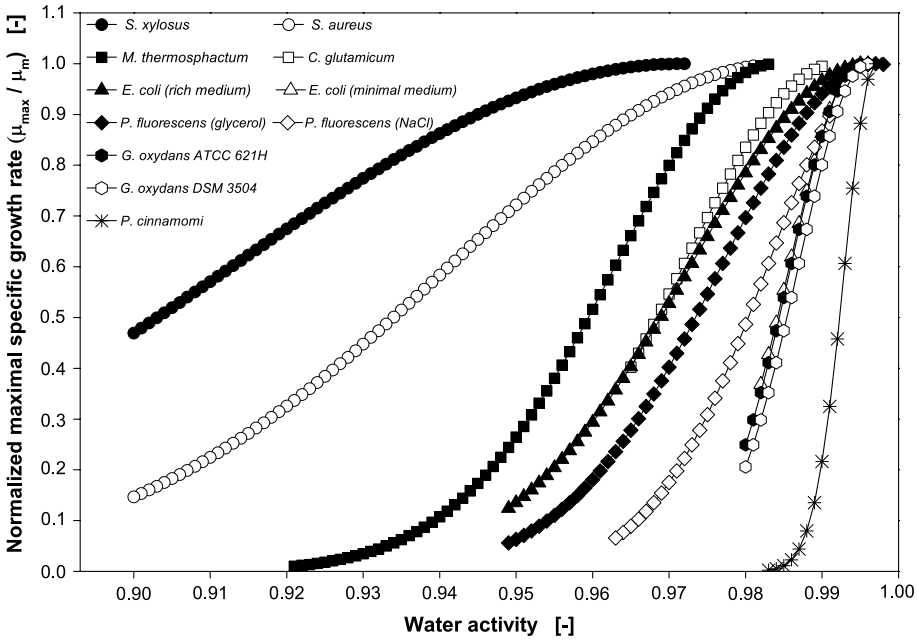

Fig. 7 Influence of water activity on the normalized maximal specific growth rates of different microorganisms fitted with the modified Davey model (Eq. 11). The maximal specific growth rates were normalized against the maximal growth rate at the optimal water activity according to the Davey model. The data for *G. oxydans* ATCC 621H and DSM 3504 are obtained from Fig. 6a, b. The parameters of the Davey model for the different microorganisms are given in Table 3

Table 3 Parameters of the modified Davey model (Eq. 11) for various microorganisms characterizing their osmotic sensitivity

Microbial strain	Fit parameters			References
	μ_m (h^{-1})	$a_{w,m}$	da_w	
G. oxydans ATCC 621H	0.45	0.995	0.009	This work (Fig. 6a)
G. oxydans DSM 3504	0.67	0.996	0.009	This work (Fig. 6b)
S. xylosus	1.1	0.972	0.058	[10]
S. aureus	1.44	0.985	0.043	[11]
M. thermosphactum	0.65	0.984	0.021	[10]
C. glutamicum	0.76	0.997	0.019	[19]
E. coli (rich medium)	2.3	0.997	0.023	[36]
E. coli (minimal medium)	0.98	0.995	0.009	[36]
P. fluorescens (glycerol)	0.39	0.998	0.02	[34]
P. fluorescens (NaCl)	0.4	0.998	0.015	[34]
P. cinnamomi	0.027	0.997	0.009	[46]

Pseudomonas fluorescens on water activities when glycerol or NaCl were used as osmotica. These experimental data were approximated with the Davey model and are illustrated in Fig. 7. It becomes clear, that, if NaCl was used as osmoticum, *P. fluorescens* responds more sensitive in comparison to growth on media with varying glycerol amounts. *Corynebacterium glutamicum* possesses an optimal specific growth rate at a water activity of 0.9983 and growths up to a water activity of 0.96, as reported by Guillouet and Engasser [19]. The most osmotic-tolerant microorganisms illustrated in Fig. 7 are *Microbacterium thermosphactum* [10], *Staphylococcus aureus* [11] and *Staphylococcus xylosus* [10] with optimal specific growth rates at water activities of 0.984, 0.985 and 0.972, respectively. Summarizing, *G. oxydans* ATCC 621H and DSM 3504 show a comparably high osmotic sensitivity under the applied experimental conditions with NaCl, KCL and $MgSO_4$ as osmotica. Presumably, the application of other osmotica or the change of the medium composition could increase *Gluconobacters* osmotic tolerance, as shown for *E. coli* and *P. fluorescens* (Fig. 7).

Conclusion

The activity of enzymes oxidizing D-glucose to gluconic acids is pH-dependent. Thus, a suitable buffer is necessary to stabilize the pH-value during cultivations of *G. oxydans* on glucose to enable process development and optimization in shake flasks. Calcium carbonate ($CaCO_3$), the commonly used buffer for cultivations of *G. oxydans*, is not convenient for laboratory-scale screening processes. Since screening often relies on optical measurements and determination of dry cell weight, the insolubility of $CaCO_3$ often hinders the analysis. Soluble buffers would solve this problem, but their application is strongly limited by the high osmotic sensitivity of *G. oxydans* ATCC 621H and DSM 3504 in comparison to other microorganisms of industrial interest. Even though only PIPPS was found to be a partially adequate alternative to the commonly used $CaCO_3$ buffer, it caused reduced cell growth and reduced respiration activity.

To improve growth and respiration activity, one option would be to reduce the medium osmolality, e.g., by decreasing the substrate and buffer concentration to 0.055 mol L^{-1}

glucose and 0.11 mol L^{-1} PIPPS. However, this option would lead to an undesirable reduction in productivity.

In essence, this study clearly points out that the osmotic sensitivity of *G. oxydans* has to be considered if high concentrations of substrate or soluble buffers are to be applied. It is important that osmolality values of >0.5 osmol kg^{-1} should not be exceeded to achieve optimal growth and product formation.

Acknowledgments This work was performed within the research network "Genomik Transfer", funded by the Federal Ministry of Research and Education, Germany (FKZ 0315632B). The authors wish to thank Stephanie Bringer and Janine Richhardt from the Institute of Bio- and Geosciences at the Research Center Jülich (Germany) as well was Wolfgang Liebl, Armin Ehrenreich and David Kostner from the Department of Microbiology at the Technological University Munich (Germany) for providing the *G. oxydans* strains ATCC 621H and DSM 3504.

References

1. Ameyama M, Matsushita K, Ohno Y, Shinagawa E, Adachi O (1981) Existence of a novel prosthetic group, PQQ, in membrane-bound, electron transport chain-linked, primary dehydrogenases of oxidative bacteria. FEBS Lett 130(2):179–183. doi:10.1016/0014-5793(81)81114-3
2. Anderlei T, Büchs J (2001) Device for sterile online measurement of the oxygen transfer rate in shaking flasks. Biochem Eng J 7(2):157–162. doi:10.1016/S1369-703X(00)00116-9
3. Anderlei T, Mrotzek C, Bartsch S, Amoabediny G, Peter CP, Büchs J (2007) New method to determine the mass transfer resistance of sterile closures for shaken bioreactors. Biotechnol Bioeng 98(5):999–1007. doi:10.1002/bit.21490
4. Anderlei T, Zang W, Papaspyrou M, Büchs J (2004) Online respiration activity measurement (OTR, CTR, RQ) in shake flasks. Biochem Eng J 17(3):187–194. doi:10.1016/S1369-703x(03)00181-5
5. Asai T (1968) Acetic Acid Bacteria: Classification and Biochemical Activities. University of Tokyo Press, Tokyo
6. Beschkov V, Velizarov S, Peeva L (1995) Some kinetic aspects and modeling of biotransformation of D-glucose to keto-d-gluconates. Bioprocess Eng 13:301–305. doi:10.1007/BF00369561
7. Brown AD (1990) Microbial water stress physiology: principles and perspectives. Wiley, Chichester
8. Brown DA, Cook RA (1981) Role of metal cofactors in enzyme regulation. Differences in the regulatory properties of the *Escherichia coli* nicotinamide adenine dinucleotide phosphate specific malic enzyme, depending on whether magnesium ion or manganese ion serves as divalent cation. Biochemistry 20(9):2503–2512. doi:10.1021/bi00512a022
9. Buchenauer A, Hofmann MC, Funke M, Büchs J, Mokwa W, Schnakenberg U (2009) Micro-bioreactors for fed-batch fermentations with integrated online monitoring and microfluidic devices. Biosens Bioelectron 24(5):1411–1416. doi:10.1016/j.bios.2008.08.043
10. Davey KR (1989) A predictive model for combined temperature and water activity on microbial-growth during the growth-phase. J Appl Bacteriol 67(5):483–488. doi:10.1111/j.1365-2672.1989.tb02519.x
11. Davey KR (1991) Applicability of the Davey (Linear Arrhenius) predictive model to the lag phase of microbial-growth. J Appl Bacteriol 70(3):253–257. doi:10.1111/j.1365-2672.1991.tb02933.x
12. Duggan PF (1977) An enzyme system requiring magnesium, calcium and potassium ions. Proc R Ir Acad B 77(19–47):449–455
13. Ellis KJ, Morrison JF (1982) Buffers of constant ionic strength for studying pH-dependent processes. Methods Enzymol 87:405–426. doi:10.1016/S0076-6879(82)87025-0
14. Funke M, Buchenauer A, Schnakenberg U, Mokwa W, Diederichs S, Mertens A, Müller C, Kensy F, Büchs J (2010) Microfluidic BioLector-Microfluidic bioprocess control in microtiter plates. Biotechnol Bioeng 107(3):497–505. doi:10.1002/Bit.22825
15. Gao L, Hu Y, Liu J, Du G, Zhou J, Chen J (2014) Stepwise metabolic engineering of *Gluconobacter oxydans* WSH-003 for the direct production of 2-keto-L-gulonic acid from D-sorbitol. Metab Eng 24:30–37. doi:10.1016/j.ymben.2014.04.003
16. Good NE, Izawa S (1972) Hydrogen ion buffers. Methods Enzymol 24:53–68. doi:10.1016/0076-6879(72)24054-X
17. Greenfield S, Claus G (1972) Nonfunctional tricarboxylic acid cycle and the mechanism of glutamate biosynthesis in *Acetobacter suboxydans*. J Bacteriol 112(3):1295–1301
18. Griffin DM (1981) Water and micobial stress. Adv Microb Ecol 5:91–136. doi:10.1007/978-1-4615-8306-6_3
19. Guillouet S, Engasser JM (1995) Sodium and proline accumulation in *Corynebacterium glutamicum* as a response to an osmotic saline upshock. Appl Microbiol Biotechnol 43(2):315–320. doi:10.1007/BF00172831
20. Gupta A, Singh VK, Qazi GN, Kumar A (2001) *Gluconobacter oxydans*: its biotechnological applications. J Mol Microbiol Biotechnol 3(3):445–456
21. Hommel R, Ahnert P (2000) Gluconobacter. Encyclopedia of food microbiology. Academic Press, London
22. Jeude M, Dittrich B, Niederschulte H, Anderlei T, Knocke C, Klee D, Büchs J (2006) Fed-batch mode in shake flasks by slow-release technique. Biotechnol Bioeng 95:433–445. doi:10.1002/bit.21012
23. Kandegedara A, Rorabacher DB (1999) Noncomplexing tertiary amines as "better" buffers covering the range of pH 3-11. Temperature dependence of their acid dissociation constants. Anal Chem 71(15):3140–3144. doi:10.1021/ac9902594
24. Kumar S, Wittmann C, Heinzle E (2004) Review: minibioreactors. Biotechnol Lett 26(1):1–10. doi:10.1023/b:bile.0000009469.69116.03
25. Lichtenthaler FW (2006) The key sugars of biomass: Availability, present non-food applications and potential industrial development lines. Biorefineries, biobased industrial processes and products. Wiley-VHC, Weinheim
26. Matsushita K, Toyama H, Adachi O (1994) Respiratory chains and bioenergetics of acetic acid bacteria. Adv Microb Physiol 36:247–301. doi:10.1016/S0065-2911(08)60181-2
27. Mille Y, Beney L, Gervais P (2005) Compared tolerance to osmotic stress in various microorganisms: towards a survival prediction test. Biotechnol Bioeng 92(4):479–484. doi:10.1002/bit.20631
28. Mori H, Kobayashi T, Shimizu S (1981) High density production of sorbose from sorbitol by fed-batch culture with DO-stat. J Chem Eng Jpn 14(1):65–70. doi:10.1252/jcej.14.65
29. Nobel PS (1983) Introduction to biophysical plant physiology, 2 edn. San Fancisco
30. Olijve W, Kok JJ (1979) Analysis of growth of *Gluconobacter oxydans* in glucose containing media. Arch Microbiol 121(3):283–290. doi:10.1007/BF00425069
31. Olijve W, Kok JJ (1979) Analysis of the growth of *Gluconobacter oxydans* in chemostat cultures. Arch Microbiol 121(3):291–297. doi:10.1007/BF00425070
32. Peña C, Galindo E, Büchs J (2011) The viscosifying power, degree of acetylation and molecular mass of the alginate produced by *Azotobacter vinelandii* in shake flasks are determined by the oxygen transfer rate. Process Biochem 46(1):290–297. doi:10.1016/j.procbio.2010.08.025

33. Po HN, Senozan NM (2001) The Henderson-Hasselbalch equation: its history and limitations. J Chem Educ 78(11):1499. doi:10.1021/ed078p1499
34. Prior BA (1978) Effect of water activity on growth and respiration of *Pseudomonas fluorescens*. J Appl Bacteriol 44(1):97–106. doi:10.1111/j.1365-2672.1978.tb00780.x
35. Raspor P, Goranovic D (2008) Biotechnological applications of acetic acid bacteria. Crit Rev Biotechnol 28(2):101–124. doi:10.1080/07388550802046749
36. Record MT Jr, Courtenay ES, Cayley DS, Guttman HJ (1998) Responses of *E. coli* to osmotic stress: large changes in amounts of cytoplasmic solutes and water. Trends Biochem Sci 23(4):143–148. doi:10.1016/S0968-0004(98)01196-7
37. Richhardt J, Luchterhand B, Bringer S, Büchs J, Bott M (2013) Evidence for a key role of cytochrome bo_3 oxidase in respiratory energy metabolism of *Gluconobacter oxydans*. J Bacteriol 195(18):4210–4220. doi:10.1128/JB.00470-13
38. Scheidle M, Dittrich B, Klinger J, Ikeda H, Klee D, Büchs J (2011) Controlling pH in shake flasks using polymer-based controlled-release discs with pre-determined release kinetics. BMC Biotechnol 11:25. doi:10.1186/1472-6750-11-25
39. Seletzky JM, Noack U, Hahn S, Knoll A, Amoabediny G, Büchs J (2007) An experimental comparison of respiration measuring techniques in fermenters and shake flasks: exhaust gas analyzer vs. RAMOS device vs. respirometer. J Ind Microbiol Biotechnol 34(2):123–130. doi:10.1007/s10295-006-0176-2
40. Shinagawa E, Ameyama M (1982) 2-Keto-D-gluconate dehydrogenase from *Gluconobacter melanogenus*, membrane-bound. Methods Enzymol
41. Shinagawa E, Matsushita K, Adachi O, Ameyama M (1981) Purification and characterization of 2-keto-D-gluconate dehydrogenase from *Gluconobacter melanogenus*. Agric Biol Chem 45(5):1079–1085. doi:10.1271/bbb1961.45.1079
42. Shinagawa E, Matsushita K, Adachi O, Ameyama M (1984) D-gluconate dehydrogenase, 2-keto-D-gluconate yielding, from *Gluconobacter dioxyacetonicus*—purification and characterization. Agric Biol Chem 48(6):1517–1522
43. Sievers M, Swings J, Garrity G, Brenner D, Krieg N, Staley J (2005) The genus gluconobacter. Springer, New York
44. Silberbach M, Maier B, Zimmermann M, Büchs J (2003) Glucose oxidation by *Gluconobacter oxydans*: characterization in shaking-flasks, scale-up and optimization of the pH profile. Appl Microbiol Biotechnol 62(1):92–98. doi:10.1007/s00253-003-1222-x
45. Sonoyama T, Tani H, Matsuda K, Kageyama B, Tanimoto M, Kobayashi K, Yagi S, Kyotani H, Mitsushima K (1982) Production of 2-keto-L-gulonic acid from D-glucose by two-stage fermentation. Appl Environ Microbiol 43(5):1064–1069
46. Sterne R, Zentmyer G, Bingham F (1976) The effect of osmotic potential and specific ions on growth of *Phytophthora cinnamomi*. GROWTH 1(1):5–10
47. Weenk G, Olijve W, Harder W (1984) Ketogluconate formation by *Gluconobacter* species. Appl Biochem Biotechnol 20(6):400–405. doi:10.1007/BF00261942
48. Weuster-Botz D (2005) Parallel reactor systems for bioprocess development. Adv Biochem Eng Biotechnol 92:125–143. doi:10.1007/b98916
49. Weuster-Botz D, Altenbach-Rehm J, Arnold M (2001) Parallel substrate feeding and pH-control in shaking-flasks. Biochem Eng J 7(2):163–170. doi:10.1016/S1369-703X(00)00117-0
50. Woods D, Duniway J (1986) Some effects of water potential on growth, turgor, and respiration of *Phytophthora cryptogea* and *Fusarium moniliforme*. Phytopathology 76(11):1248–1254
51. Zavrel M, Bross D, Funke M, Büchs J, Spiess AC (2009) High-throughput screening for ionic liquids dissolving (ligno-)cellulose. Bioresour Technol 100(9):2580–2587. doi:10.1016/j.biortech.2008.11.052
52. Zou X, Guo X, Sun M (2009) pH control strategy in a shaken mini bioreactor for polysaccharide production by medicinal mushroom *Phellinus linteus* and its anti-hyperlipemia activity. Bioprocess Biosyst Eng 32(2):277–281. doi:10.1007/s00449-008-0241-5